TiO_2 alterations with natural aging: Unveiling the role of nitric acid on NIR reflectance

Riccardo Paolini[1]*, Mohamad Sleiman[2,3,4], MariaPia Pedeferri[5,6], Maria Vittoria Diamanti[5,6]*

[1] Politecnico di Milano, Department of Architecture, Built environment and Construction engineering, Via Ponzio 31, 20133 – Milan, Italy
[2] Lawrence Berkeley National Laboratory, Indoor Environment Group, 1 Cyclotron Road MS 70-108B, Berkeley, CA, USA
[3] Clermont Université, ENSCCF, Institut de Chimie de Clermont-Ferrand, BP 10448, F-63000 Clermont-Ferrand, France
[4] CNRS, UMR 6296, ICCF, BP 80026, F-63177 Aubière, France
[5] Politecnico di Milano, Department of Chemistry, Materials and Chemical Engineering "G. Natta", Via Mancinelli 7, 20131 Milan, Italy
[6] INSTM - National Interuniversity Consortium of Materials Science and Technology, Via G. Giusti 9, 50121 Florence, Italy

* Corresponding authors:
Riccardo Paolini, email: riccardo.paolini@polimi.it – address: Via Ponzio 31, 20133 Milan, Italy – Tel. +390223996015
Maria Vittoria Diamanti, email: mariavittoria.diamanti@polimi.it – address: Via Mancinelli 7, 20131 Milan, Italy – Tel. +390223993137

Abstract

The development of photoactive materials with self-cleaning and depolluting qualities is a hot topic in materials science, given their impact on several technologies, in a wide range of contexts of applications. Anatase phase titanium dioxide (TiO_2) is the largest used photocatalyst, with increasing applications ranging from air quality control to renewable energies, to green building materials for zero energy communities. Yet, it is partially transmissive in the near infrared (NIR), which negatively affects the solar reflectance of TiO_2 containing materials. In this contribution we describe an unexpected increase in anatase near infrared (NIR) reflectance observed during environmental exposure. We unveil its complex mechanisms, based on the contact with nitric acid generated by NO_x photocatalytic degradation, which causes partial reduction and decrease in crystallinity to TiO_2. This may open the way for introducing multiple environmentally beneficial effects on TiO_2 pollutants degradation, self-cleaning, and energy performance.

Keywords: TiO_2; near-infrared reflectance; nitric acid; aging; P25.

Introduction

Over the last century, the growth of world's population has mostly concerned urban areas, which are responsible for 71% of global energy-related carbon emissions [1]. A manifold positive contribution to climate change mitigation and in the improvement of air quality of built environments can be provided by a smart performance-based design of urban envelope components, mainly roofing [2]. These should retain a surface temperature close to the ambient temperature under the sun, which reduces the turbulent sensible heat released into the urban environment [3], and possibly display also some de-polluting features. This objective may be achieved with vegetative surfaces such as green roofs, that are not always a technically viable and cheap solution [4], or with man-made materials having high solar reflectance and thermal emittance, widely known as cool materials [5]. A relevant option is that of titanium dioxide (TiO_2), that may be integrated in building materials in order to spread its beneficial effect on the largest surface area possible [6–8]. With its high refractive index, rutile TiO_2 is the largest used white pigment, but it is partially transmissive in the near infrared wavelength range, which negatively affects solar reflectance.

Nevertheless, the benefits in using TiO_2 – and in particular the anatase phase – rely, first of all, on the UV-activated photocatalytic degradation of pollutants mediated by TiO_2, which can mitigate pollution arising from industrial sources, heating and transportation [6]. These may be either organic – industrial wastewaters, volatile organic compounds (VOCs) emitted by exhausts, combustion gases, etc. [9–11] – or inorganic – nitrogen oxides [12–14]. Moreover, changes in wettability upon UV irradiation lead to a superhydrophilic state which, coupled with photocatalysis, results in the so called self-cleaning effect [15]. In such mechanism, the bridging groups used by atmospheric contaminants and soot to adhere to surfaces are partially photomineralized and subsequently washed away by water, allowing

materials to retain a cleaner and more reflective surface over time [16–18]. In addition, reducing the impact of aging on the optical-radiative performance of built environment surfaces has a strong influence on the thermal comfort and energy consumption of buildings [19,20], and therefore on the urban microclimate [21]. The actual performance of these technologies is particularly important as prospects indicate that the cooling needs of buildings will increase, worldwide, from 4.4% to 35% of the total heating and cooling needs by 2050, and to 61% by 2100. The largest increases are expected in India, where the residential cooling energy consumption of 2050 is foreseen to be approximately ten times that of 2010 [22].

Another relevant area where TiO_2 is used as an electrode is that of Dye-Sensitized Solar Cells (DSSCs), that still face issues because of aging upon environmental exposure [23,24]. Therefore, a deeper understanding of the modifications over the whole solar spectrum of TiO_2 upon aging is desirable also on the power generation side, in addition to that of energy saving.

Here we present a novel effect of anatase phase TiO_2, which we first noticed during long-term environmental [25] and laboratory accelerated exposure campaigns [26]: an increase in reflectance in the near infrared (NIR) wavelength range upon material aging. We reproduced this effect in the laboratory, envisioning the mechanisms responsible for such unexpected variation.

Experimental

Materials

Two distinct sets of samples were used in two campaigns of outdoor long-term exposure. One focused on uncoated commercial fiber-reinforced mortars, containing TiO_2 in mass in the mortar formulation, constituting the outer skin of pre-cast thermally insulated panels produced by PIZ SpA [25,27]. The mortar formulation, with special reference to the type and content of photocatalytic admixture, was previously optimized [28]; composition is reported in Table 1. The second campaign considered commercial bitumen roofing membrane reinforced with polyester fabric and coated with siloxane paint, provided by Index SpA. The latter material was also used in laboratory experimental tests. The coating consisted of a water-based siloxane paint for cementitious surfaces and slated membranes, containing calcium carbonate as an extender, as well as dispersant, wetting, and antifoam additives. Both a standard coating and a photoactive one were tested: the former contained rutile TiO_2 white pigments of 300 nm minimum size, the latter contained both the same pigmentary rutile and anatase TiO_2 with 15 nm average particle dimension. Samples for outdoor exposure were cut in 10 cm x 10 cm squares from a membrane sheet with a thickness of 0.5 cm, while for subsequent investigations smaller samples 4 cm x 4 cm were cut.

Methods

Long-term outdoor exposure: The natural aging started in Milan in April 2012, with three replicates per product for each exposure condition. Fiber-reinforced mortars were vertically exposed, facing north and south. The roofing membranes were exposed low sloped (i.e., 1.5% slope, that is the minimum for flat roofs) [29]. The solar spectral reflectance was characterized for unexposed samples, and each six months; here we report the results after two years.

Table 1. Standard mortar composition – in photocatalytic mortars, 5% of anatase nanoparticles by cement weight is added [27].

Portland cement (CEM I 42.5 R)	555 kg/m^3
Silica sand	1110 kg/m^3
W/C ratio	0.56
Expansive admixture	33 kg/m^3
Waterproof additive	22 kg/m^3
Glass fibers	20 kg/m^3
Antifoaming admixture	1 kg/m^3

Accelerated exposure: Accelerated exposure consisted in immersing membrane samples in different aqueous solutions for 24 h, focusing on two acid solutions – HNO_3 and H_2SO_4 – to reproduce the contact of the materials with sulfuric or nitric acids generated by pollution or by TiO_2 itself as byproduct of its photoactivity [14,30,31]. The list of solutions employed is given in Table 2. For each combination, two standard samples and two photoactive samples were used. Tests were repeated on AEROXIDE® TiO_2 P25 powders, as representative of a standard material commonly utilized in studies on TiO_2 photoinduced properties.

Powders were mixed with either deionized water or a solution containing 1% by weight of HNO_3 in proportions 1:3. After 18 h the mixture was partially dried on a hot plate at 50°C, obtaining a white paste. Five samples were then prepared for spectrophotometry measurements by depositing a uniform layer of 1 g of TiO_2 paste on a polyester transparent sheet.

Table 2. Solutions and immersion times utilized in the accelerated exposure procedures for standard and photoactive membranes

Solution	Concentration [% by weight]	pH	Duration
H_2O	100%	6	24 h
HNO_3	0.25% - 0.5% – 1%	1	24 h
H_2SO_4	0.1%	1	24 h

Photocatalytic activity: Photocatalytic activity of membranes coated with photoactive paint was tested before and after HNO_3 treatment by using a dye discoloration method. Specifically, rhodamine B – a dye with magenta hue – was chosen, as it is commonly accepted and utilized to test the efficiency of photocatalytic materials as representative of organic pollutants. Samples were immersed in an aqueous solution of the dye with concentration 10^{-5} M for 3 h, dried and then exposed to artificial light simulating the solar spectrum (Osram Vitalux lamp, 300 W) with UV intensity at 370 nm of 1 mW cm^{-2}. Their

color before and after irradiation was measured by reflectance spectrophotometry, using a Konica Minolta CM-2600d spectrophotometer. The software Spectramagic NX was then used to convert reflectance information into color coordinates L* a* b* in the color space CIELab, as defined by the Commission Intérnationale de l'Éclairage [32,33]. Rhodamine B degradation was correlated to the decrease in the a* (red) coordinate of color, representing a loss of intensity in red and therefore a discoloration of the dye.

Analytical techniques: For XRD (X-ray diffraction) analyses a Philips PW 1830-Cu Kα radiation instrument was employed (40 kV applied tension, 0.5◦/min scan rate).

UV-Vis-NIR reflectance measurements were carried out between 300 and 2500 nm, with a spectral resolution of 5 nm, with a Perkin Elmer Lambda 950 spectrometer, equipped with a 150 mm integrating sphere. The slit in the Vis range was set to 2 nm from 300 to 860 nm, and in servo mode for the rest of the scan, with a characterized area of approximately 15 mm x 15 mm between 1500 and 2500 nm. For the naturally exposed samples, just the central portion of each was characterized, while for those immersed in acid, two non-overlapping spots per sample were measured. The error bars in the graphs identify the range. Broadband values were then computed considering the solar spectral irradiance distribution for clear sky conditions and air mass equal to 1 [34]. ρ_s and ρ_{h2} are, respectively, the solar reflectance and the broadband reflectance in the range between 1500 and 2500 nm.

A Perkin Elmer Frontier IR was used for ATR-FTIR characterizations (Attenuated Total Reflectance-Fourier Transform InfraRed spectroscopy).

Results

Outdoor exposure campaigns were first carried out on commercial materials: fiber-reinforced mortars [27] and bituminous roofing membranes coated with siloxane paint, both exposed in triplicate and both in a standard formulation and in a photoactive one, the latter containing anatase TiO_2. The reflectance of samples with standard composition decreased, especially in the wavelength range between 400 and 2200 nm, consistently with previous work [29,35], due to the complex of UV aging, soot and other particulate deposition (Figure S1, Supporting Information). Yet, after natural aging, the reflectance of anatase containing samples increased in the last portion of the NIR wavelength range (Figure 1, S1, and S2, Supporting Information). The overall trend in broadband NIR reflectance (700-2500 nm) still indicated a decrease, as the trend inversion only occurred at approximately 1500 nm, but above such threshold the trend was monotonously increasing with respect to the initial optical properties of the material (Figure S3, Supporting Information).

Further analyses were aimed at reproducing the observed effect in laboratory: we focused such investigations on membranes, as the simpler composition and smoother surface would allow to produce less artifacts. Pristine membranes were immersed for 24 h in diluted solutions of nitric acid, sulfuric acid, or tap water: each was aimed at simulating compounds either present in the environment or possibly generated by TiO_2 photocatalytic activity, with which the membrane surface would therefore come into contact. In particular, nitric acid and sulfuric acid may be generated by the degradation of main atmospheric pollutants NO_x and SO_2, which produce NO_3^- and SO_4^{2-}, respectively. Equations 1 and 2 describe the case of nitrates formation, as more likely to be observed in current environments where large quantities of NO_x are released [14,30,31,36].

$$H_2O/O_2 \xrightarrow{TiO_2+h\upsilon} HO^{\bullet}{}_{(ads)} + O_2^{\bullet-}{}_{(ads)} \quad (1)$$

$$NO_x \xrightarrow{HO^{\bullet}+O_2^{\bullet-}} NO_3{}^{-}{}_{(ads)} \xrightarrow{H_2O} HNO_{3(ads)} \quad (2)$$

The contact with organic substances or particulate matter were not considered as possible causes of NIR reflectance increase, as their presence on the surface would cause the opposite modification in surface properties [35]. Moreover, during immersion tests, sulfuric acid was found to cause exceeding damage to the paint, which was not observed with natural aging, and was therefore discarded from subsequent investigations (Figure S3, Supporting Information).

The effects induced by such immersions were evaluated by attenuated total reflectance Fourier transform infrared reflectance (ATR-FTIR) and X-ray diffraction (XRD).
Immersion of membranes in both acid solutions increased their reflectance between 1500 nm and 2500 nm, while immersion in water did not give any change in their NIR optical response, nor in their composition (Figure 1b and S3, Supporting Information). Both ATR-FTIR (Figure 1c) and XRD measurements (Figure S4, Supporting Information) on membranes coated with photoactive paint only revealed a partial disappearance of calcium carbonate ($CaCO_3$) constituents of the paint (main peak at 29.3° in XRD, and peaks at 712, 872, 1390 and 1798 cm^{-1} in ATR-FTIR). This is compatible with the acid environment in which the material was processed, but at the same time cannot be considered as responsible of the observed increase in NIR reflectance, given the high reflectivity of $CaCO_3$. Therefore, no relevant information could be drawn on the source of the effect observed.

The deposition of inorganic nitrates and sulfates on the material surface was also discarded owing to two reasons. First, in absence of anatase phase TiO_2 no variation was observed, which makes sense in outdoor exposure where acids formation is ascribed to photocatalytic reactions driven by anatase, but is not compatible with the hypothesis of nitrates or sulfates deposition once the material is artificially immersed in acids (Figure S5, Supporting Information). Moreover, the result of surface interactions of the material with nitric acid is stable: on subjected samples aged in HNO_3 and further immersed for 24 h in water, the increase in NIR reflectance was not cancelled, nor further increased, while sulfates and especially nitrates are generally highly soluble in water. The effect observed with the environmental exposure was also persistent, already after the first months of aging.

This led us to hypothesize the occurrence of chemical modification of anatase due to contact with acid solutions. In fact, strong acids on anatase phase TiO_2 may yield to an increase in porosity and surface area and the stable adsorption of nitrates, together with anatase surface protonation and increase in Ti^{3+} states [37,38].

To isolate the sole effect of TiO_2 in predominant anatase phase, tests were repeated on commercial TiO_2 P25 powders, containing approximately 70 to 80% of anatase and 20 to 30% of rutile [39]. An analogous increase in NIR reflectance was seen on TiO_2 P25 powders immersed in HNO_3 compared with those immersed in deionized water (Figure 2a).

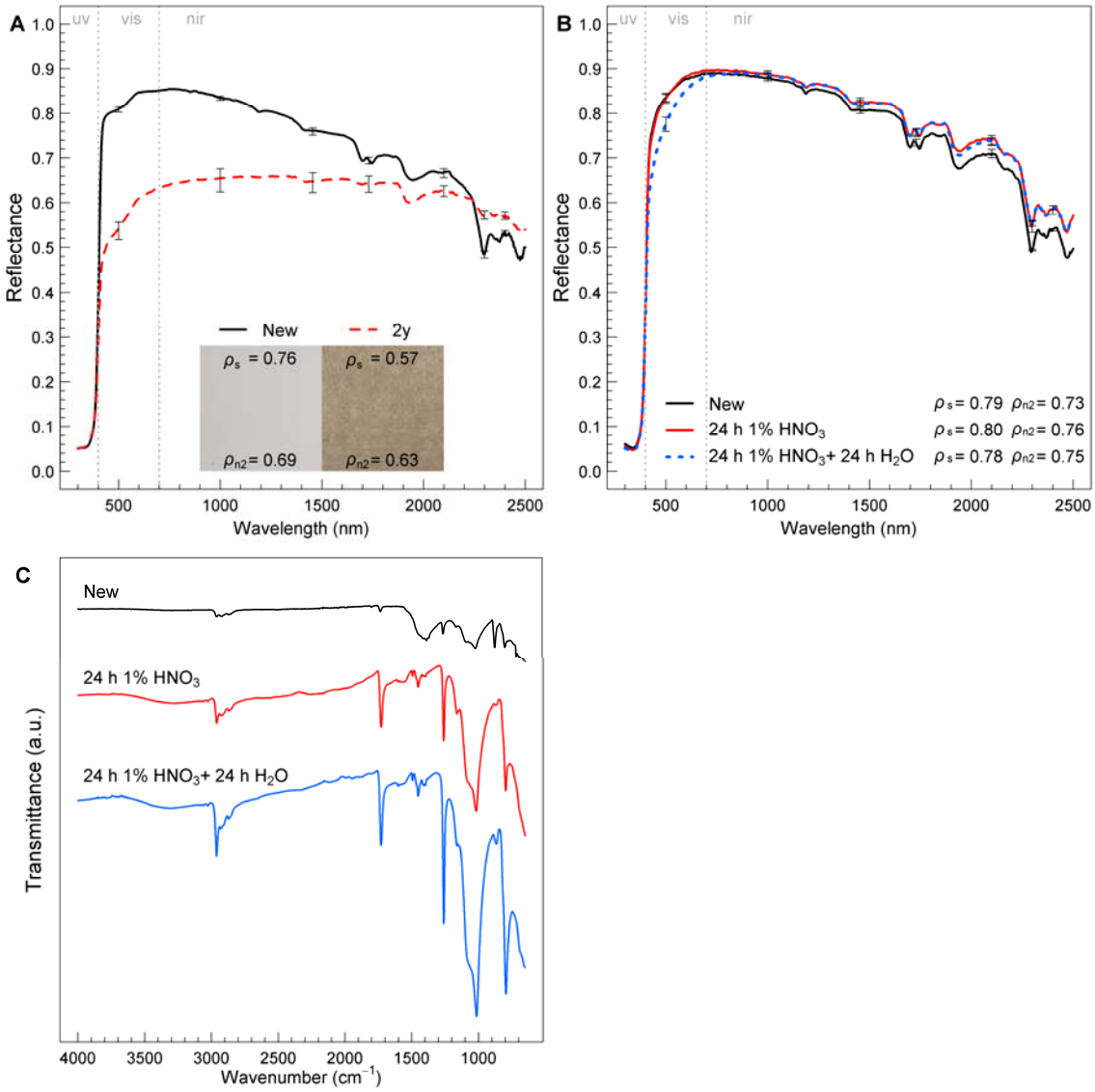

Figure 1. (A) Solar spectral reflectance of modified bitumen roofing membranes coated with a commercial paint containing anatase TiO_2, before (new) and after 2 years (2y) of natural aging. (B) The same membranes before (new), after immersion in nitric acid (24 h 1% HNO_3), and then after additional immersion in deionized water (24 h 1% HNO_3 + 24 h H_2O). Insets visualize the aspect of specimens before and after exposure. (C) ATR-FTIR transmittance (arbitrary units) of the same membranes before and after immersion in nitric acid and then in deionized water.

Powders were then characterized by X-ray diffraction (XRD, Figure 2b) and scanning electron microscopy (SEM, Figure 3). No relevant variation was observed in the general aspect of powder clusters after immersion in water or in nitric acid, indicating that effects observed on NIR reflectance were not originated by alterations in the aggregation state of particles at the microscopic and submicroscopic level, although nanoscale morphological variations may actually appear on single nanoparticles. XRD characterization demonstrated that the immersion in nitric acid causes a decrease in the crystallinity of TiO_2 P25 powders, as attested by the decrease in both anatase and rutile main peaks intensity (at 25.2° and 27.6°, respectively), with rutile almost complete disappearance. The anatase peak also showed a

clear broadening, with an increase in full width at half maximum by 20%, indicating a decrease in crystallite size (Figure 2b – see Supplementary Material for detailed information). Since in the materials on which this effect was observed the photoactive admixture was only anatase, our attention will now focus on this polymorph.

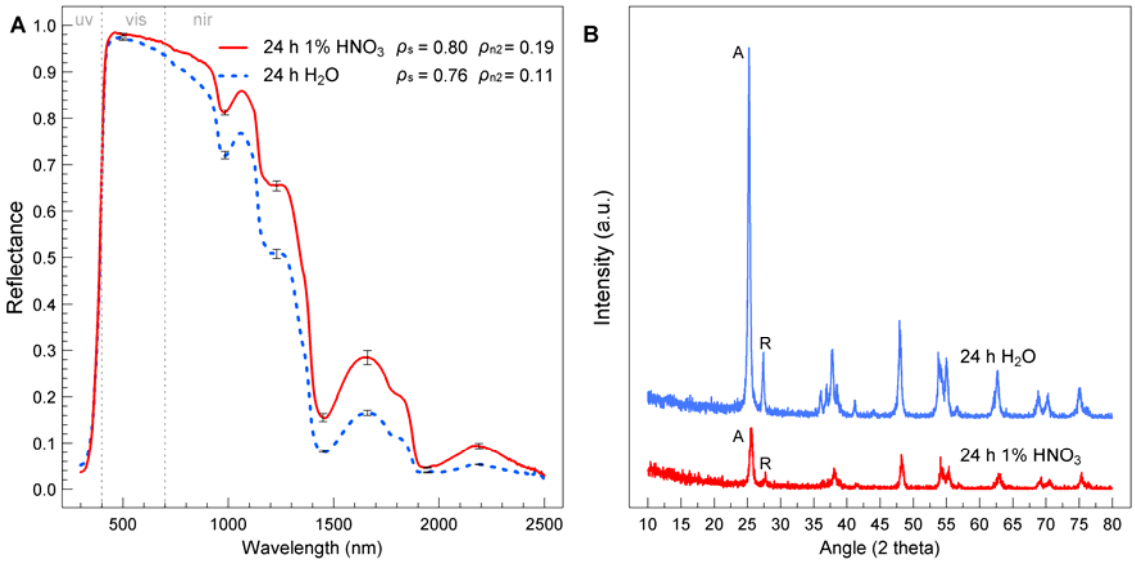

Figure 2. (A) Solar spectral reflectance of P25 powder after 24 h of immersion in HNO_3 or in deionized water. ρ_s and ρ_{n2} are, respectively, the solar reflectance and the broadband reflectance in the range between 1500 and 2500 nm. The error bars identify the range. (B) XRD intensity peaks of same powders, main anatase peak (A) at 25.2°, main rutile peak (R) at 27.6°.

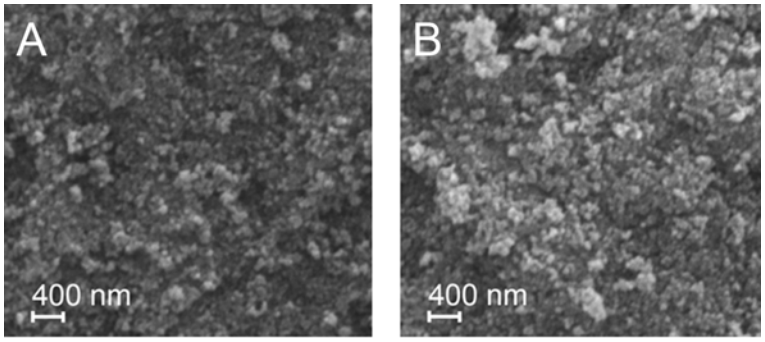

Figure 3. (A) SEM of P25 after immersion in DI water. (B) SEM of P25 after immersion in HNO_3. Magnifications 40 kX.

Finally, the influence on photocatalytic activity of the optical and structural modifications identified on the TiO_2 P25 samples was investigated. These measurements only represent a preliminary investigation, as more in-depth tests are being evaluated for a more precise characterization. In spite of the preliminary character of these results, the method chosen allowed to identify an alteration of the powders photocatalytic activity, causing a decrease in efficiency by approximately 15-20% (Table 3). This is likely to be ascribed to the strong decrease in TiO_2 crystallinity.

Table 3. Photocatalytic efficiency assessed with rhodamine B test. Dye discoloration percentages at different irradiation times in presence of membranes coated with photoactive paints, after 24 h immersion either in water (label: M-H) or in nitric acid (label: M-N).

Material	Percent discoloration				
	1 h	2 h	3 h	4 h	5 h
M-H	35.5	44.4	53.5	55.7	57.2
M-N	27.2	36.6	42.3	45.2	48.1

Discussion

We hypothesize the following reaction mechanism to explain the variations in the optical behavior of anatase TiO_2 in presence of HNO_3 on the surface, which in natural environments can be produced by the photodegradation of NO_x by anatase and consequent hydrolyzation of NO_3^- to HNO_3 (Figure 4) [14]:

1. The acid environment causes on TiO_2 morphological effects: increase in surface area; chemical ones: hydroxylation, protonation, adsorption of NO_3^-, increase in Ti^{3+} surface defects; and structural ones: partial degradation of TiO_2 crystal structure, as revealed by XRD peaks loss of intensity and simultaneous broadening [37,40].
2. Such effects may yield to higher optical density, and therefore reduce transmittance and increase backscattering. The recorded increase in reflectance is proportional to the wavelength (Figure 1b, Figure 2a), and higher for longer exposure to nitric acid (Figure S2a, Supporting Information).

Surface modifications of titania pastes upon treatment with nitric acid have been previously shown to increase the absorbance in the 400-800 nm wavelength range, enhancing the light-harvesting effectiveness of DSSCs, and the incident photon-to-current conversion efficiency because of increased forward scattering [41]. It was also found that the NO_3^- ions produced after immersion in HNO_3 may coat the TiO_2 and block the path of backward electron transfer [42]. Our results in the visible wavelength range are consistent with the literature. The increase in the reflectance in the near infrared wavelength range is interesting as that portion of the spectrum is not used for energy conversion by DSSCs activated by visible light, and an increased back-scattering might contribute to reduce the surface temperature of DSSCs, and therefore increase their efficiency.

The increase in reflectance observed in the laboratory can be translated into an actual reduction of surface temperatures by approximately 2°C in peak conditions, for instance for a highly insulated roof. This is still a small change, but already relevant for the building performance. However, there is large potential for the improvement of methods to retain - and in the specific case to increase - a high solar reflectance, which may lead to much larger reduction in surface temperature, and therefore in cooling loads. Furthermore, materials with high NIR reflectance are also reported to be less impacted by aging than materials with same solar reflectance, but higher response at shorter wavelengths [29], namely where the detrimental and degrading action of UV and black carbon is strongest [35].

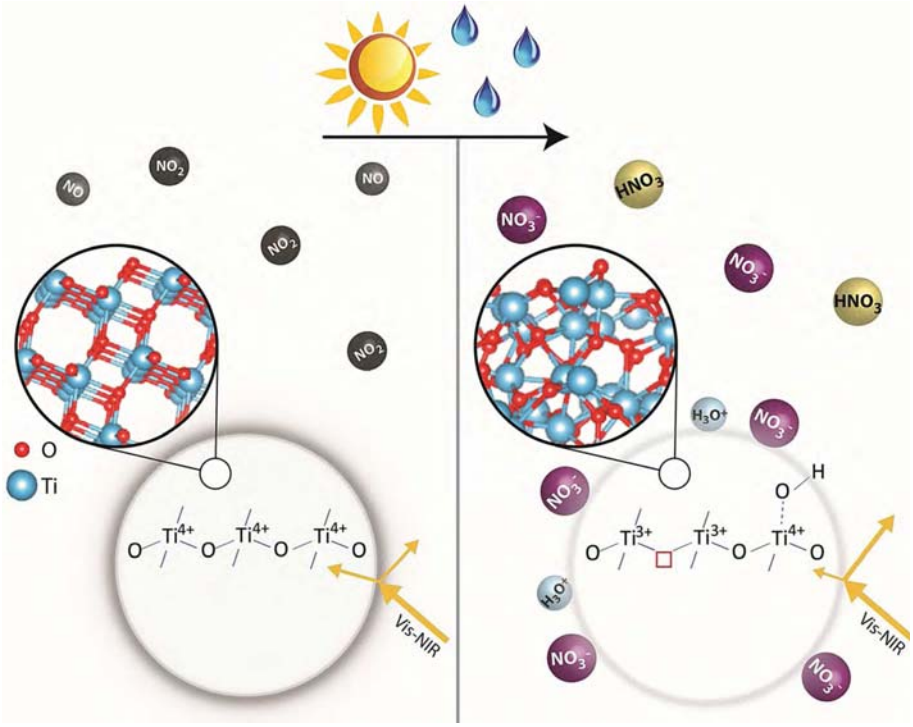

Figure 4. Schematic representation of reactions occurring at the surface of anatase phase TiO_2. Left: TiO_2 in presence of NO_x, crystal structure and atoms coordination highlighted (facet 101 was chosen as representative in the structure inset) [40]. The yellow arrows represent light hitting the TiO_2 surface and being reflected or transmitted. Right: as a consequence of sunlight (UV) irradiation in humid environment, NO_x are converted to NO_3^- which in turn are hydrolyzed to HNO_3; nitrates adsorb on the protonated TiO_2 surface resulting from the acid environment, with increase in oxide defect density Ti^{3+} and decrease in crystallinity (amorphous structure inset) [40].

Conclusions

On account of these observations, we can conclude that this study opens the door for HNO_3 treatment of TiO_2 as a method to develop TiO_2 pigments for self-cleaning construction materials with improved optical-radiative properties. This is supported by the maintaining of all the cited properties also after rinsing the material with water: thus, modified materials could be safely used after eliminating HNO_3, which would be harmful to the environment and to the surrounding materials. Finally, the HNO_3 treatment proved to be only partially detrimental towards the TiO_2 photocatalytic activity, likely on account of a lower crystallinity and partial occupation of active sites by NO_3^-, which is an adverse effect that needs to be addressed and minimized. Yet, surface protonation would help improving two fundamental aspects in the development of highly efficient photocatalysts. First, the material formulation may be improved thanks to an easier dispersion of particles, reducing tendency to agglomeration. Then, its selectivity may be enhanced, specifically towards the adsorption of alkaline pollutants – for instance, tobacco alkaloids – potentially increasing photocatalytic activity against specific species. These aspects open the way to new advances in the field of photocatalytic and self-cleaning materials.

Acknowledgements

This work was in part supported by Politecnico di Milano & Agenzia delle Entrate (Italian Revenue Agency) with the project "Cinque per mille junior - Rivestimenti fluorurati avanzati per superfici edilizie ad alte prestazioni". The authors gratefully acknowledge Nicola Bonato of Index S.p.a. for having supplied the roofing membranes, and the PIZ division of Zecca Prefabbricati S.p.A. for the fibre-reinforced mortars. The authors also thankfully acknowledge Marta Rossini (Politecnico di Milano) who contributed to the UV-Vis-NIR measurements on the membranes; and Maria Grazia Garavaglia (Perkin Elmer Italia) for the ATR-FTIR measurements.

References

[1] C. Rosenzweig, W. Solecki, S.A. Hammer, S. Mehrotra, Cities lead the way in climate-change action., Nature. 467 (2010) 909–11. doi:10.1038/467909a.

[2] H. Akbari, C. Cartalis, D. Kolokotsa, A. Muscio, A.L. Pisello, F. Rossi, et al., Local climate change and urban heat island mitigation techniques – the state of the art, Journal of Civil Engineering and Management. 22 (2015) 1–16. doi:10.3846/13923730.2015.1111934.

[3] A.M. Rizwan, L.Y.C. Dennis, C. Liu, A review on the generation, determination and mitigation of Urban Heat Island, Journal of Environmental Sciences. 20 (2008) 120–128. doi:10.1016/S1001-0742(08)60019-4.

[4] J. Sproul, M.P. Wan, B.H. Mandel, A.H. Rosenfeld, Economic comparison of white, green, and black flat roofs in the United States, Energy and Buildings. 71 (2014) 20–27. doi:10.1016/j.enbuild.2013.11.058.

[5] M. Santamouris, Cooling the cities – A review of reflective and green roof mitigation technologies to fight heat island and improve comfort in urban environments, Solar Energy. 103 (2014) 682–703. doi:10.1016/j.solener.2012.07.003.

[6] A. Fujishima, X. Zhang, D. Tryk, TiO2 photocatalysis and related surface phenomena, Surface Science Reports. 63 (2008) 515–582. doi:10.1016/j.surfrep.2008.10.001.

[7] H. Xu, S. Ouyang, L. Liu, P. Reunchan, N. Umezawa, J. Ye, Recent advances in TiO 2 -based photocatalysis, Journal of Materials Chemistry A. 2 (2014) 12642. doi:10.1039/C4TA00941J.

[8] F. Pacheco-Torgal, M.V. Diamanti, A. Nazari, C. Goran-Granqvist, Nanotechnology in Eco-Efficient Construction. Materials, Processes and Applications, Woodhead Publishing Ltd, 2013.

[9] K. Demeestere, J. Dewulf, B. De Witte, A. Beeldens, H. Van Langenhove, Heterogeneous photocatalytic removal of toluene from air on building materials enriched with TiO2, Building and Environment. 43 (2008) 406–414. doi:10.1016/j.buildenv.2007.01.016.

[10] S. Lorencik, Q.L. Yu, H.J.H. Brouwers, Design and performance evaluation of the functional coating for air purification under indoor conditions, Applied Catalysis B: Environmental. 168-169 (2015) 77–86. doi:10.1016/j.apcatb.2014.12.012.

[11] M.R. Hoffmann, S.T. Martin, W. Choi, D.W. Bahnemann, Environmental Applications of Semiconductor Photocatalysis, Chemical Reviews. 95 (1995) 69–96. doi:10.1021/cr00033a004.

[12] J. Ângelo, L. Andrade, L.M. Madeira, A. Mendes, An overview of photocatalysis phenomena applied to NOx abatement., Journal of Environmental Management. 129 (2013) 522–39. doi:10.1016/j.jenvman.2013.08.006.

[13] B.Y. Lee, A.R. Jayapalan, M.H. Bergin, K.E. Kurtis, Photocatalytic cement exposed to nitrogen oxides: Effect of oxidation and binding, Cement and Concrete Research. 60 (2014) 30–36. doi:10.1016/j.cemconres.2014.03.003.

[14] O. Rosseler, M. Sleiman, V.N. Montesinos, A. Shavorskiy, V. Keller, N. Keller, et al., Chemistry of NOx on TiO2 Surfaces Studied by Ambient Pressure XPS: Products, Effect of UV Irradiation, Water, and Coadsorbed K(.)., The Journal of Physical Chemistry Letters. 4 (2013) 536–41. doi:10.1021/jz302119g.

[15] R. Wang, K. Hashimoto, A. Fujishima, M. Chikuni, E. Kojima, A. Kitamura, et al., Light-induced amphiphilic surfaces, 388 (1997) 431–432.

[16] M. Smits, C. kit Chan, T. Tytgat, B. Craeye, N. Costarramone, S. Lacombe, et al., Photocatalytic degradation of soot deposition: Self-cleaning effect on titanium dioxide coated cementitious materials, Chemical Engineering Journal. 222 (2013) 411–418. doi:10.1016/j.cej.2013.02.089.

[17] M. Smits, D. Huygh, B. Craeye, S. Lenaerts, Effect of process parameters on the photocatalytic soot degradation on self-cleaning cementitious materials, Catalysis Today. 230 (2014) 250–255. doi:10.1016/j.cattod.2013.10.001.

[18] J. Bogdan, A. Jackowska-Tracz, J. Zarzyńska, J. Pławińska-Czarnak, Chances and limitations of nanosized titanium dioxide practical application in view of its physicochemical properties, Nanoscale Research Letters. 10 (2015) 57. doi:10.1186/s11671-015-0753-2.

[19] H. Akbari, R. Levinson, L. Rainer, Monitoring the energy-use effects of cool roofs on California commercial buildings, Energy and Buildings. 37 (2005) 1007–1016. doi:10.1016/j.enbuild.2004.11.013.

[20] A.L. Pisello, F. Cotana, The thermal effect of an innovative cool roof on residential buildings in Italy: Results from two years of continuous monitoring, Energy and Buildings. 69 (2014) 154–164. doi:10.1016/j.enbuild.2013.10.031.

[21] A.H. Rosenfeld, H. Akbari, J.J. Romm, M. Pomerantz, Cool communities: strategies for heat island mitigation and smog reduction, Energy and Buildings. 28 (1998) 51–62. doi:10.1016/S0378-7788(97)00063-7.

[22] M. Santamouris, Cooling the buildings – past, present and future, Energy and Buildings. 128 (2016) 617–638. doi:10.1016/j.enbuild.2016.07.034.

[23] M. Berginc, U.O. Krašovec, M. Topič, Outdoor ageing of the dye-sensitized solar cell under different operation regimes, Solar Energy Materials and Solar Cells. 120 (2014) 491–499. doi:10.1016/j.solmat.2013.09.029.

[24] C.H. Kwak, J.H. Baeg, I.M. Yang, K. Giribabu, S. Lee, Y.S. Huh, Degradation analysis of dye-sensitized solar cell module consisting of 22 unit cells for thermal stability:

Raman spectroscopy study, Solar Energy. 130 (2016) 244–249. doi:10.1016/j.solener.2016.02.017.

[25] M.V. Diamanti, R. Paolini, M. Zinzi, M. Ormellese, M. Fiori, M.P. Pedeferri, Self-cleaning ability and cooling effect of TiO 2 -containing mortars, in: NSTI-Nanotech 2013, Washington, USA, 2013: pp. 716–719.

[26] S. Wang, J. Zhang, L. Liu, F. Yang, Y. Zhang, Evaluation of cooling property of high density polyethylene (HDPE)/titanium dioxide (TiO2) composites after accelerated ultraviolet (UV) irradiation, Solar Energy Materials and Solar Cells. 143 (2015) 120–127. doi:10.1016/j.solmat.2015.06.032.

[27] M.V. Diamanti, R. Paolini, M. Rossini, A.B. Aslan, M. Zinzi, T. Poli, et al., Long term self-cleaning and photocatalytic performance of anatase added mortars exposed to the urban environment, Construction and Building Materials. 96 (2015) 270–278. doi:10.1016/j.conbuildmat.2015.08.028.

[28] M.V. Diamanti, M. Ormellese, M. Pedeferri, Characterization of photocatalytic and superhydrophilic properties of mortars containing titanium dioxide, Cement and Concrete Research. 38 (2008) 1349–1353. doi:10.1016/j.cemconres.2008.07.003.

[29] R. Paolini, M. Zinzi, T. Poli, E. Carnielo, A.G. Mainini, Effect of ageing on solar spectral reflectance of roofing membranes: natural exposure in Roma and Milano and the impact on the energy needs of commercial buildings, Energy and Buildings. 84 (2014) 333–343. doi:10.1016/j.enbuild.2014.08.008.

[30] D. Osborn, M. Hassan, H. Dylla, Quantification of Reduction of Nitrogen Oxides by Nitrate Accumulation on Titanium Dioxide Photocatalytic Concrete Pavement, Transportation Research Record: Journal of the Transportation Research Board. 2290 (2012) 147–153. doi:10.3141/2290-19.

[31] R. Atkinson, D.L. Baulch, R.A. Cox, J.N. Crowley, R.F. Hampson, R.G. Hynes, et al., Evaluated kinetic and photochemical data for atmospheric chemistry: Volume I - gas phase reactions of O_x, HO_x, NO_x and SO_x species, Atmospheric Chemistry and Physics. 4 (2004) 1461–1738. doi:10.5194/acp-4-1461-2004.

[32] R.W.G. Hunt, The Specification of Colour Appearance. I. Concepts and Terms, Color Research & Application. 2 (1977) 55–68. doi:10.1002/col.5080020202.

[33] M. V. Diamanti, B. Del Curto, M. Pedeferri, Interference colors of thin oxide layers on titanium, Color Research & Application. 33 (2008) 221–228. doi:10.1002/col.20403.

[34] R. Levinson, H. Akbari, P. Berdahl, Measuring solar reflectance—Part I: Defining a metric that accurately predicts solar heat gain, Solar Energy. 84 (2010) 1717–1744. doi:10.1016/j.solener.2010.04.018.

[35] M. Sleiman, T.W. Kirchstetter, P. Berdahl, H.E. Gilbert, S. Quelen, L. Marlot, et al., Soiling of building envelope surfaces and its effect on solar reflectance – Part II: Development of an accelerated aging method for roofing materials, Solar Energy Materials and Solar Cells. 122 (2014) 271–281. doi:10.1016/j.solmat.2013.11.028.

[36] S.-J. Yuan, J.-J. Chen, Z.-Q. Lin, W.-W. Li, G.-P. Sheng, H.-Q. Yu, Nitrate formation from atmospheric nitrogen and oxygen photocatalysed by nano-sized titanium dioxide., Nature Communications. 4 (2013) 2249. doi:10.1038/ncomms3249.

[37] A.L. Goodman, E.T. Bernard, V.H. Grassian, Spectroscopic Study of Nitric Acid and Water Adsorption on Oxide Particles: Enhanced Nitric Acid Uptake Kinetics in the Presence of Adsorbed Water, The Journal of Physical Chemistry A. 105 (2001) 6443–6457. doi:10.1021/jp003722l.

[38] K.-H. Park, E.M. Jin, H.B. Gu, S.E. Shim, C.K. Hong, Effects of HNO3 treatment of TiO2 nanoparticles on the photovoltaic properties of dye-sensitized solar cells, Materials Letters. 63 (2009) 2208–2211. doi:10.1016/j.matlet.2009.07.034.

[39] B. Ohtani, O.O. Prieto-Mahaney, D. Li, R. Abe, What is Degussa (Evonik) P25? Crystalline composition analysis, reconstruction from isolated pure particles and photocatalytic activity test, Journal of Photochemistry and Photobiology A: Chemistry. 216 (2010) 179–182. doi:10.1016/j.jphotochem.2010.07.024.

[40] S. Manzhos, G. Giorgi, K. Yamashita, A density functional tight binding study of acetic acid adsorption on crystalline and amorphous surfaces of titania., Molecules (Basel, Switzerland). 20 (2015) 3371–88. doi:10.3390/molecules20023371.

[41] T. Watson, C. Charbonneau, D. Bryant, D. Worsley, T. Watson, C. Charbonneau, et al., Acid Treatment of Titania Pastes to Create Scattering Layers in Dye-Sensitized Solar Cells, International Journal of Photoenergy. 2012 (2012) 1–8. doi:10.1155/2012/637839.

[42] H.S. Jung, J.K. Lee, S. Lee, K.S. Hong, H. Shin, Acid adsorption on TiO2 nanoparticles - An electrochemical properties study, Journal of Physical Chemistry C. 112 (2008) 8476–8480. doi:10.1021/jp711689u.